Molecular Cell *23*, 709–721, September 1, 2006 ©2006 Elsevier Inc. DOI 10.1016/j.molcel.2006.08.010

A Family of Diverse Cul4-Ddb1-Interacting Proteins Includes Cdt2, which Is Required for S Phase Destruction of the Replication Factor Cdt1

Jianping Jin,[1,3] Emily E. Arias,[2,3] Jing Chen,[1] J. Wade Harper,[1,*] and Johannes C. Walter[2,*]
[1] Department of Pathology
[2] Department of Biological Chemistry and Molecular Pharmacology
Harvard Medical School
Boston, Massachusetts 02115

Summary

Cul4 E3 ubiquitin ligases contain the cullin 4 scaffold and the triple β propeller Ddb1 adaptor protein, but few substrate receptors have been identified. Here, we identify 18 *D*db1- and *C*ul4-*a*ssociated *f*actors (DCAFs), including 14 containing WD40 repeats. DCAFs interact with multiple surfaces on Ddb1, and the interaction of WD40-containing DCAFs with Ddb1 requires a conserved "WDXR" motif. DCAF2/Cdt2, which is related to *S. pombe* Cdt2, functions in *Xenopus* egg extracts and human cells to destroy the replication licensing protein Cdt1 in S phase and after DNA damage. Depletion of human Cdt2 causes rereplication and checkpoint activation. In *Xenopus*, Cdt2 is recruited to replication forks via Cdt1 and PCNA, where Cdt1 ubiquitylation occurs. These studies uncover diverse substrate receptors for Cul4 and identify Cdt2 as a conserved component of the Cul4-Ddb1 E3 that is essential to destroy Cdt1 and ensure proper cell cycle regulation of DNA replication.

Introduction

Ubiquitin-mediated proteolysis is a central mechanism by which regulatory proteins and their consequent signaling events are controlled. Attachment of ubiquitin to a target protein proceeds through a cascade involving an E1 activating enzyme, an E2 conjugating enzyme, and an E3 ubiquitin ligase (Pickart, 2004). E3s provide specificity to ubiquitylation reactions by bridging substrates and E2s. Cullin-RING-based E3s (CRLs) constitute a major subclass of RING finger E3s (Petroski and Deshaies, 2005). Seven cullins have been identified in human cells, each of which functions as a "scaffold" around which the active ubiquitin ligase assembles. All cullins interact with an E2 binding RING finger protein (Rbx1 or Rbx2) through their C-terminal domain and with substrate receptors via the N terminus (Zheng et al., 2002; Petroski and Deshaies, 2005).

The best-understood CRL is the SCF complex, which employs Skp1 to link Cul1 with members of the F-box family of substrate receptors (Bai et al., 1996). F-box proteins interact with Skp1 through an N-terminal F-box motif and with substrates through C-terminal WD40 or leucine-rich repeats (reviewed in Petroski and Deshaies [2005]). Similarly, Cul2 and Cul5 complexes employ the Skp1-like protein Elongin C to interact with SOCS-box proteins while Cul3 employs BTB proteins as receptors. Together, these CRLs may assemble more than 200 distinct E3s.

In contrast with the cullins described above, receptors for Cul4A and Cul4B are poorly understood. Cul4A and Cul4B interact through their N terminus with Ddb1 (damage-specific DNA binding protein 1). Ddb1 appears to function as a Skp1-like adaptor, as it can interact with at least three potential substrate receptors in human cells (Ddb2, CSA, Det1-Cop1), and with Cdt2 in *S. pombe*. In human cells, Cul4-Ddb1^{Ddb2} promotes the ubiquitylation of histone H3, histone H4 (Wang et al., 2006), and the xeroderma pigmentosum (XP) group C protein, XP-C (Sugasawa et al., 2005) to regulate their activity. Ddb2 is mutated in humans of the XP-complementation group E subtype (Kapetanaki et al., 2006). In contrast, Cul4-Ddb1^{CSA} and Cul4-Ddb1$^{Det1\text{-}Cop1}$ promote proteolysis of CSB and c-*jun*, respectively (Wertz et al., 2004; Groisman et al., 2006). Both CSA and CSB are mutated in patients with Cockayne syndrome. Finally, *S. pombe* Cul4-Ddb1^{Cdt2} is required for the degradation of Spd1, an inhibitor of ribonucleotide reductase that is destroyed at the onset of S phase and after DNA damage (Liu et al., 2005). Interestingly, Ddb2, Cop1, CSA, and *S. pombe* Cdt2 contain WD40 repeats, which are frequently used in CRLs such as the SCF to bind substrates (Petroski and Deshaies, 2005).

Another substrate of Cul4-Ddb1 is the DNA replication factor Cdt1, although no substrate receptor for Cdt1 has been identified. In G1, Cdt1 cooperates with the origin recognition complex (ORC) and Cdc6 to recruit MCM2-7 into a prereplication complex or pre-RC (the "licensing" reaction) (Blow and Dutta, 2005). In S phase, the MCM2-7 helicase is activated, and it travels away from the origin, leading to pre-RC disassembly. In vertebrates, origin refiring in S, G2, and M phase is prevented because de novo MCM2-7 loading is prohibited, primarily through the inhibition of Cdt1 activity via Geminin and ubiquitin-mediated proteolysis. Available evidence suggests that Cdt1 ubiquitylation and degradation involve Ddb1 and Cul4 in humans, *Xenopus*, and *C. elegans* (Zhong et al., 2003; Higa et al., 2003; Hu et al., 2004; Nishitani et al., 2006; Arias and Walter, 2006). In S phase, Cul4-Ddb1-dependent Cdt1 ubiquitylation occurs exclusively on chromatin in a manner that is dependent on DNA replication (Arias and Walter, 2005, 2006; Nishitani et al., 2001, 2006). Cdt1 contains a highly conserved PCNA interaction motif (called a PIP box), which is required for its destruction in S phase (Arias and Walter, 2006; Senga et al., 2006; Nishitani et al., 2006). Ddb1 is recruited to chromatin during replication initiation, suggesting that Cdt1 and its E3 ubiquitin ligase both bind to the replication fork via PCNA, leading to ubiquitin transfer (Arias and Walter, 2006). Interestingly, human Cdt1 is rapidly destroyed in response to DNA damage by a proteolysis pathway that requires Cdt1's PIP box, PCNA, Cul4, and Ddb1 (Higa et al., 2003; Hu et al., 2004; Hu and Xiong, 2006; Nishitani et al., 2006; Senga et al., 2006).

*Correspondence: wade_harper@hms.harvard.edu (J.W.H.); johannes_walter@hms.harvard.edu (J.C.W.)
[3] These authors contributed equally to this work.

Structural analysis of Ddb1 in complex with the simian paramyxovirus SV5 protein—which co-opts Ddb1-Cul4 to promote STAT degradation—shows that Ddb1 contains three seven-bladed β propellers (designated βPA, βPB, and βPC), potentially providing a large surface area for recruitment of additional specificity factors (Li et al., 2006). SV5 contacts βPC while Cul4 binds βPB. Using a proteomic approach, we identified 18 previously unknown human *D*db1- and *C*ul4-*a*ssociated *f*actors (DCAFs), the majority of which contain WD40 repeats. WD40-containing DCAFs employ "WDXR" motifs to bind Ddb1, and many DCAFs, like SV5, make contacts with βPC. Furthermore, we found that DCAF2, the apparent vertebrate ortholog of *S. pombe* Cdt2, is required for destruction of Cdt1 during S phase and after DNA damage in human cells and in *Xenopus* egg extracts, through a mechanism that involves Cdt1 and PCNA-dependent recruitment of Cul4-Ddb1^{Cdt2} to chromatin. These experiments provide insight into the composition of the Cul4-Ddb1 ligase family and shed light on the mechanism by which cells restrict DNA replication to a single round per cell cycle.

Results

Identification of DCAFs, Candidate Substrate Receptors for the Cul4-Ddb1 Ubiquitin Ligase

To search for Ddb1-associated proteins, 293T cells expressing endogenous levels of Flag-HA-Ddb1 (Figure 1A) were subjected to tandem affinity purification (TAP). SDS-PAGE analysis revealed a number of Ddb1-associated proteins absent from control samples (Figure 1B), the identities of which were determined by mass spectrometry. Several previously identified Cul4-Ddb1-interacting proteins, including Cul4A, Cul4B, all eight subunits of the COP9 signalosome, CSA, Det1, Ddb2, and Cop1 were identified, indicating the presence of physiological Ddb1 partners (Figure 1C). In addition, 18 previously unidentified human Ddb1-interacting proteins were found, which we generally refer to as DCAFs (Figure 1C). Interestingly, like CSA, Ddb2, and Cop1, 14 of the DCAFs contained WD40 repeats (Figure 1C). One of these, DCAF2, is the closest human relative of the *S. pombe* protein Cdt2, which interacts with Ddb1 (Liu et al., 2005). DCAF2 is 26% identical and 44% similar to *Sp*Cdt2, and we will refer to the human protein as *Hs*Cdt2. Metazoan homologs of Cdt2 each contain seven WD40 repeats (data not shown), suggesting they assemble into a classical seven-bladed propeller. DCAF1 was previously identified as VprBP, a protein that interacts with the Vpr protein from human immunodeficiency virus (Zhang et al., 2001), but its connection to Ddb1 remained unknown. Five additional interaction domains were identified in DCAFs (Figure 1C): a calmodulin binding (IQ) domain in DCAF6, tetratricopeptide repeat (TPR) domains in DCAF9, a SOF motif in DCAF13, bromodomains in DCAF14, and a Lissencephaly type-1-like homology motif (LisH) in DCAF1. Like Det1, four Ddb1-associated proteins (DCAF15–17 and Dda1) lack known protein interaction domains (Figure 1C). Dda1, although a Ddb1 interaction protein, was not designated as a DCAF because it interacts with multiple Ddb1-DCAF complexes (Ning Zheng, personal communication) and therefore is unlikely to serve as a substrate receptor.

Validation of Ddb1-Interacting Proteins

To validate our TAP results, vectors expressing 15 DCAF proteins (DCAFs 1, 3–12, 14–17, and *Hs*Cdt2/DCAF2), as well as Dda1, Ddb2, CSA, and Det1, were cotransfected into 293T cells in combination with vectors expressing Flag-Cul4A, Flag-Cul4B, and Flag-HA-Ddb1 (or Flag-Ddb1) and tested for interaction (Figure 1E and see Figure S1B in the Supplemental Data available with this article online). All DCAF proteins tested were found to interact with Ddb1 with an efficiency comparable to that seen with Ddb2, CSA, and Det1, and they also interacted with Cul4A (and, in many cases, Cul4B) (Figure 1E and Figure S1B). In addition, we found that endogenous Ddb1 interacts with endogenous *Hs*Cdt2 and with DCAF1 in coimmunoprecipitation experiments (Figure 1D). These data greatly expand the number of known Ddb1- and Cul4-interacting proteins, as summarized in Figure S1A.

Distinct Modes of Interaction between Ddb1 and Its Interacting Proteins

While Ddb1 shares the adaptor function of Skp1, it is structurally more complex and contains three seven-bladed β propellers (βPA, βPB, and βPC) (Li et al., 2006). While Ddb1 is known to bind the viral SV5 protein through the "top" face of βPC and Cul4 through the "bottom" face of βPB, as defined by Li et al., (2006) (Figure 2A), it is not clear whether other Ddb1-associated proteins use the same or distinct surfaces to bind Ddb1.

To examine this question, we generated four Ddb1 mutants in βPA and βPC, which encompass conserved single residues or clusters of conserved residues on the top face of βPC and the bottom face of βPA (Figure 2A). Vectors encoding Ddb1 mutants were coexpressed with a variety of DCAF proteins as well as Dda1, CSA, Ddb2, and Det1, and interactions were tested by coprecipitation (Figure 2B and Figure S1C). The results, summarized in Figure 2C, revealed that different surfaces in Ddb1 are required for interaction with different classes of DCAF proteins. Thus, *Hs*Cdt2; Det1; DCAFs 1, 3, 5, 8, and 11; and CSA each required at least one of the three sets of residues mutated on the surface of βPC, although these proteins display clear differences in their requirements for these βPC residues (Figure 2C). For example, while Det1, DCAF1, and DCAF8 required only the M910/L912/Y913 cluster (Figure S1C, lanes 6–10, 16–20, and 33–37), *Hs*Cdt2 required this cluster as well as the E840/E842 cluster (Figure 2B, lanes 1–5). For CSA, mutation of W953 resulted in a substantial reduction in binding but the M910/L912/Y913 and E840/E842 clusters were not required (Figure S1C, lanes 48–52). DCAF3 and DCAF5 required all three sets of residues on βPC (Figure S1C, lanes 1–5 and 38–42). In contrast, Ddb2, DCAF12, and Dda1 did not require any of the residues examined in βPC (Figure 2B, lanes 5–10; Figure S1C, lanes 11–15 and 43–47). Strikingly, Dda1 was found to require a conserved cluster of residues (Y316/D318/N319) on the bottom face of βPA, revealing that Ddb1 also uses βPA to interact with proteins (Figures 2A–2C). GST alone did not associate with Ddb1 (Figure S1C, lanes 21–26), indicating the specificity of this approach. In summary, the majority of Ddb1-associated proteins interact with Ddb1 through distinct

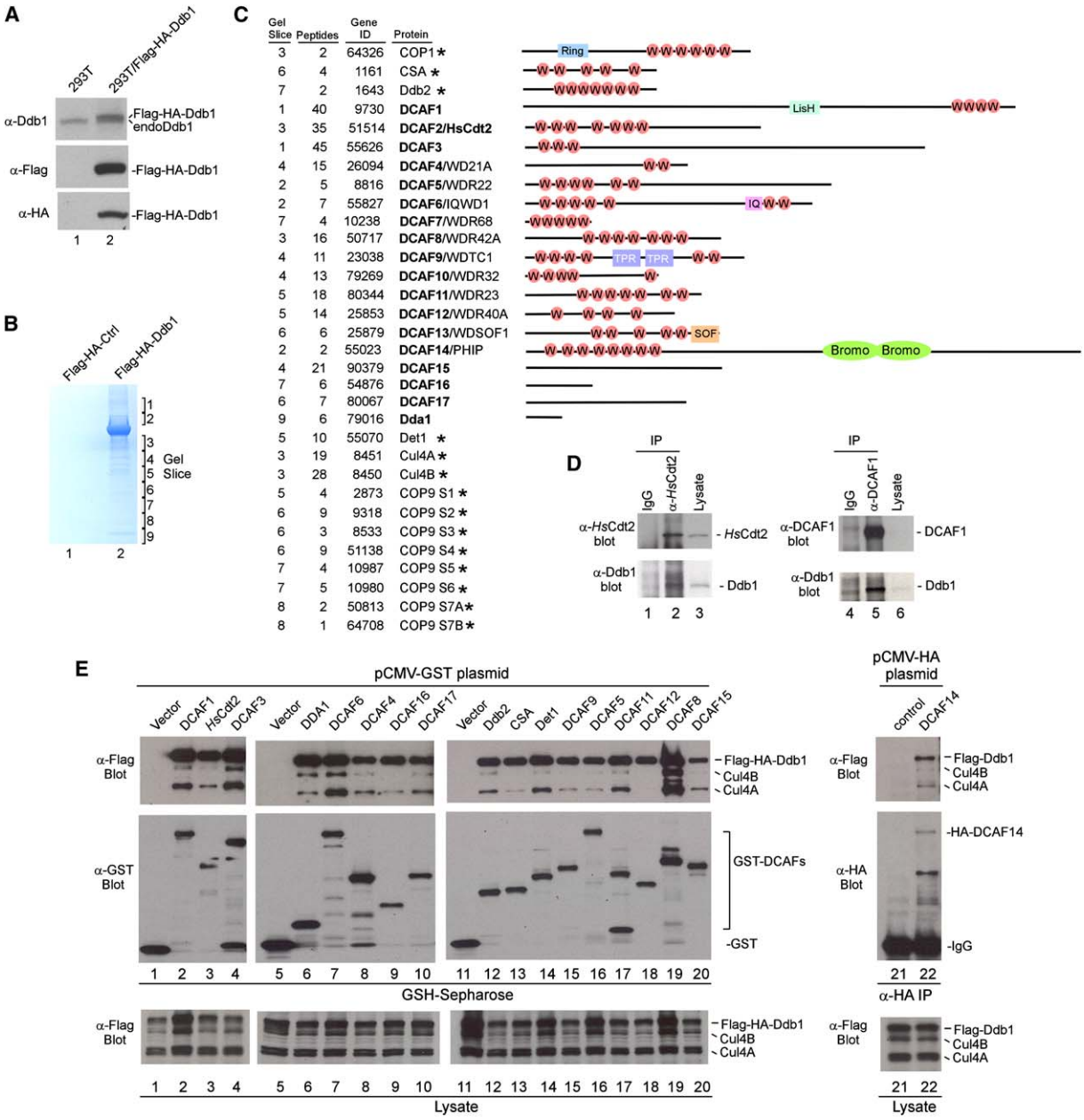

Figure 1. Identification of DCAFs

(A) Cell extracts from 293T cells or 293T cells stably expressing Flag-HA-Ddb1 were immunoblotted using α-Ddb1, α-Flag, and α-HA antibodies.

(B) Large-scale Ddb1 complexes isolated by TAP were subjected to SDS-PAGE on a 4%–12% gradient gel prior to Coomassie staining. Gel slices submitted for mass spectrometry are indicated.

(C) Ddb1-associated proteins identified by mass spectrometry are shown along with the number of peptides identified and their domain structures. Proteins previously identified in Ddb1 complexes are indicated by an asterisk.

(D) Endogenous *Hs*Cdt2 and DCAF1 were immunoprecipitated from 293T cell extracts and immunoblotted for Ddb1.

(E) Validation of interaction between DCAF proteins, Ddb1, and Cul4. pCMV-GST-DCAF expression plasmids (1.5 μg) were cotransfected with vectors expressing Flag-Cul4A, Flag-Cul4B, and Flag-HA-Ddb1 (1 μg) in 293T cells. Cell lysates were subjected to GST pull-down and blotted with α-Flag antibodies or α-GST or directly blotted with α-flag (lower panel). For DCAF14 (right panel), pCMV-HA-DCAF14, Flag-Cul4A, Flag-Cul4B, and Flag-Ddb1 expression plasmids were used for transfection and the resulting cell lysates were used for immunoprecipitation with α-HA resin.

clusters of conserved residues located on βPA or βPC of Ddb1 (Figure 2C). Interestingly, Det1 and SV5—which both lack WD40 repeats—nevertheless require residues located in βPC to bind Ddb1 (Li et al., 2006) (Figure S1C), suggesting that this pocket is used to bind structurally distinct classes of proteins.

WDXR Motifs in WD40-Containing DCAFs Are Required for Ddb1 Binding

We next sought to identify elements within WD40-containing DCAF proteins that facilitate interaction with Ddb1. Through comparative sequence analysis, we found that 15 of 16 WD40-containing Ddb1 binding

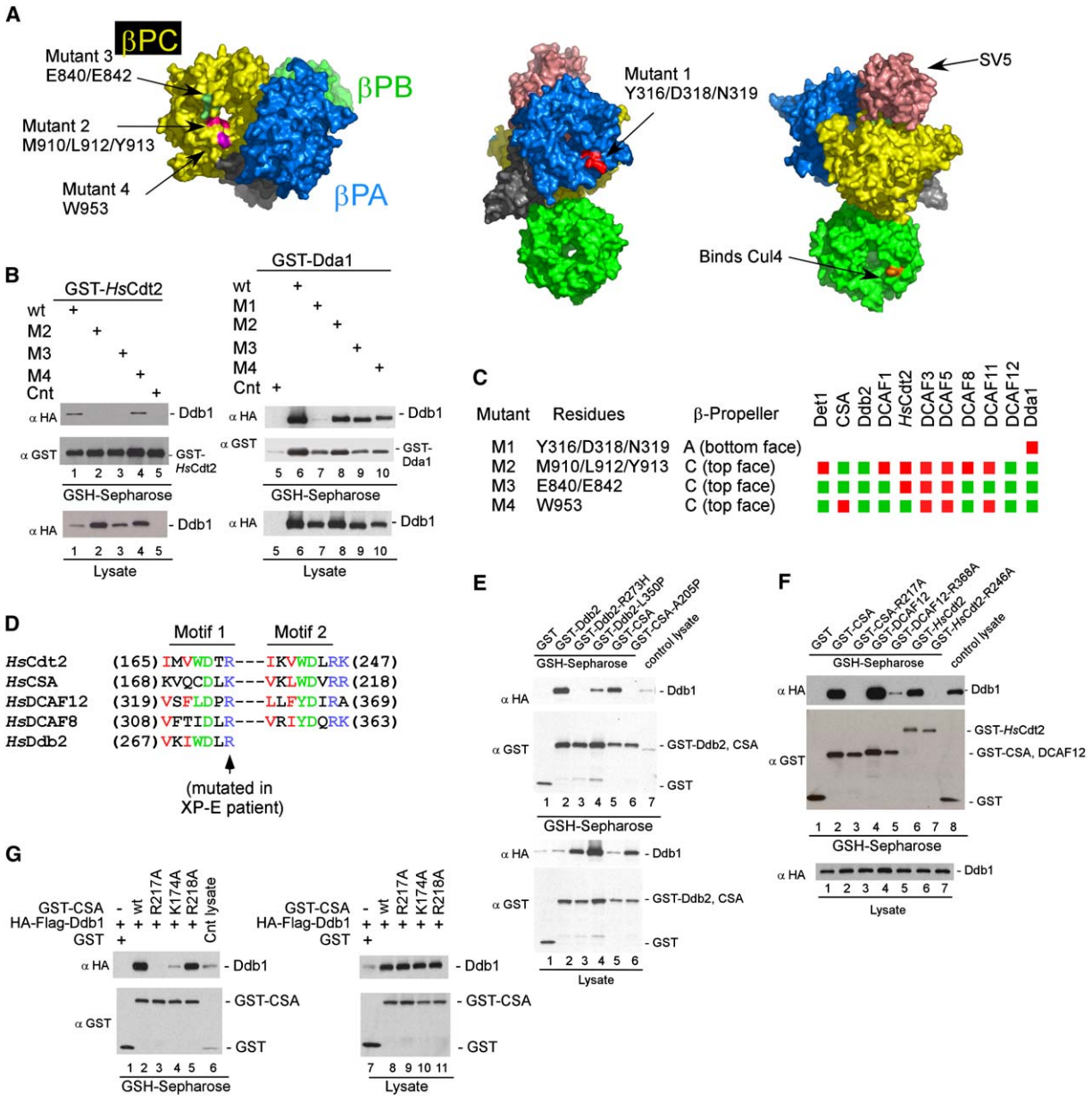

Figure 2. DCAF and Cul4 Proteins Associate with Diverse Conserved Surfaces in Ddb1

(A) Structure of Ddb1 and its complex with the viral SV5 protein (Li et al., 2006), depicting the mutations examined for interaction with DCAF proteins (βPA, blue; βPB, green; βPC, yellow; and SV5, salmon). Mutated residues are indicated.

(B and C) Effect of Ddb1 mutations on binding to *Hs*Cdt2 and Dda1 is examined in (B). After coexpression with wild-type or mutant HA-Ddb1 proteins, GST-*Hs*Cdt2 and GST-Dda1 were retrieved using GSH-Sepharose and proteins immunoblotted using α-HA or α-GST. (C) summarizes the results of an analysis of several DCAF proteins with Ddb1 mutants (Figure S1C). Green squares indicate little or no effect on binding, while red indicates a partial or complete loss of binding.

(D) Alignment of tandem WDXR motif in CSA, *Hs*Cdt2, DCAF8, DCAF12, and Ddb2. Conserved hydrophobic residues are in red, the conserved "WD" sequence in green, and conserved basic residues in blue.

(E–G) Mutations in the WDXR motifs of DCAF proteins block association with Ddb1. pCMV plasmids expressing the indicated DCAF proteins were cotransfected with Ddb1-HA-Flag and GST pull-down experiments performed as described in (B).

proteins contain an internal WD40 repeat in which the Trp-Asp dipeptide characteristic of the WD40 repeat (sometimes Tyr-Asp, Ile-Asp, or Trp-Cys in DCAFs) is followed by an X-Arg dipeptide and occasionally an X-Lys dipeptide (Figure 2D and Figures S2A and S2E). We refer to this motif as the WDXR motif to emphasize its presence within the WD40 motif itself, but we note that Trp-Asp is not absolutely conserved. In 12 of 16 cases, DCAF proteins contained two WDXR motifs positioned in tandem WD40 repeats (Figure 2D and Figures S2A and S2E). Modeling of *Hs*Cdt2 and CSA structures revealed that the arginine (or lysine) residue within this motif is located on an exposed surface on the bottom face of the β propeller, while the hydrophobic residue, tryptophan in these cases, is buried (Figures S2C and S2D). Consistent with an important functional role, these

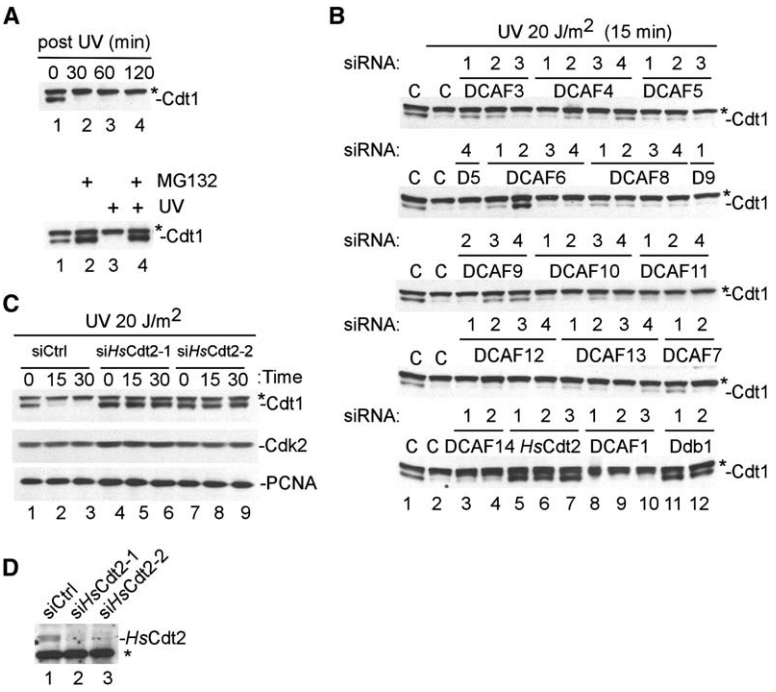

Figure 3. RNAi Screening Identifies *Hs*Cdt2 as a Protein Required for UV-Dependent Cdt1 Turnover

(A) Degradation of Cdt1 in response to UV is blocked by MG132. Cdt1 abundance was examined after UV irradiation by immunoblotting (top panel) in the presence (6 hr) or absence of MG132 (20 μg/ml). *, crossreacting protein that serves as a loading control.

(B) An RNAi screen for DCAF proteins involved in Cdt1 degradation. Two to four siRNAs targeting the indicted genes, or control siRNA, were transfected into HeLa cells, and, 72 hr later, cells were UV irradiated (20 J/m^2). After 15 min, cells were lysed and immunoblotted with α-Cdt1.

(C) Turnover of Cdt1 in response to UV treatment is blocked by *Hs*Cdt2 depletion. HeLa cells were transfected with a control siRNA or with two independent siRNAs targeting *Hs*Cdt2 and assayed at the indicated times, as in (A). α-Cdk2 and α-PCNA are loading controls.

(D) Independent siRNAs against *Hs*Cdt2 reduce its abundance. Extracts from cells transfected with the indicated siRNAs were immunoblotted with α-*Hs*Cdt2.

motifs were fully conserved in zebrafish and *Drosophila* orthologs of the DCAF proteins, and in the case of *Hs*Cdt2 were also conserved in *S. pombe* Cdt2 (Figures S2A and S2B and data not shown).

Interestingly, the arginine in the WDXR motif in Ddb2 is mutated (R273H; Figure 2D; Figure S2A) in an XP-complementation group E patient (Kapetanaki et al., 2006). This mutation abolishes binding of Ddb2 to Ddb1 (Chen et al., 2001 and Figure 2E, lane 3), indicating that R273 in Ddb2 is important for interaction with Ddb1. Further mutational analysis of other DCAF proteins indicated that CSA, DCAF12, and *Hs*Cdt2 each require the arginine in the second WDXR motif for interaction with Ddb1 (R217, R368, and R246, respectively) (Figure 2F). We also found that mutation of the corresponding residue in DCAF8 (R362; Figure 2D) substantially reduces interaction with Ddb1 (Figure S2H). We also tested the contribution of the first WDXR motif in CSA (K174A) and DCAF8 (R314A). Mutation of the basic residue in the first motif largely abrogated binding (Figure 2G and Figure S2H), suggesting that both WDXR motifs within the tandem arrangement contribute to the interaction with Ddb1. However, mutation of the arginine immediately following the second WDXR motif in CSA (R218A) had no effect on the interaction with Ddb1 (Figure 2G), suggesting that the position of the basic residue following the WD40 repeats is critical. Interestingly, a mutation previously seen in the CSA gene from a patient with Cockayne syndrome (A205P), located internally in the same WD40 repeat as the second WDXR motif (Cao et al., 2004) (Figures S2A and S2D), also blocks Ddb1 binding (Figure 2E, lane 6). Although additional structural features are likely to be important for recognition of Ddb1, these data indicate an important role for basic residues within the WDXR motif for interaction of WD40-containing DCAF proteins with Ddb1.

*Hs*Cdt2 Is Required for Degradation of the Replication Licensing Protein Cdt1 in Response to DNA Damage

To examine whether any DCAF proteins might be required for degradation of Cdt1, we systematically examined the requirements for 14 WD40-containing DCAF proteins in DNA-damage-induced Cdt1 destruction using RNAi in HeLa cells. Cdt1 was degraded with a half-life of less than 15 min after UV irradiation, consistent with previous experiments, and this degradation was blocked by the proteasome inhibitor MG132 (Figure 3A) or by depletion of Ddb1 (Figure 3B, bottom panel, compare lane 2 with lanes 11 and 12) (Higa et al., 2003; Hu et al., 2004). MG132 or Ddb1 depletion also increased the steady-state abundance of Cdt1 above that found in the absence of damage (Figure 3A, lower panel, compare lanes 1 and 2; Figure 3B, bottom panel, compare lane 1 with lanes 11 and 12). Thus, Ddb1 siRNA likely inhibited not only UV-induced destruction but also the S phase destruction of Cdt1, as previously reported (Nishitani et al., 2006). Strikingly, three independent siRNAs targeting *Hs*Cdt2 blocked UV-induced Cdt1 destruction and caused Cdt1 to accumulate above the level seen in the unirradiated cells (Figure 3B, bottom panel, compare lanes 1 and 2 with lanes 5–7). In no other case did all the siRNAs prevent UV-induced Cdt1 destruction, and the effect seen with DCAF6 siRNA #2 appeared to be an off-target activity, as RT-PCR analysis indicated that all four siRNAs targeting DCAF6 produced similar degrees of mRNA knockdown (Figure S2F). We cannot rule out that other DCAFs play a role in Cdt1 destruction. However, given the fact that our method of performing siRNA knockdown has an average success rate of >50% (our unpublished data), we consider this unlikely. The effects of *Hs*Cdt2 depletion with two independent siRNAs (Figure 3D) revealed that Cdt1

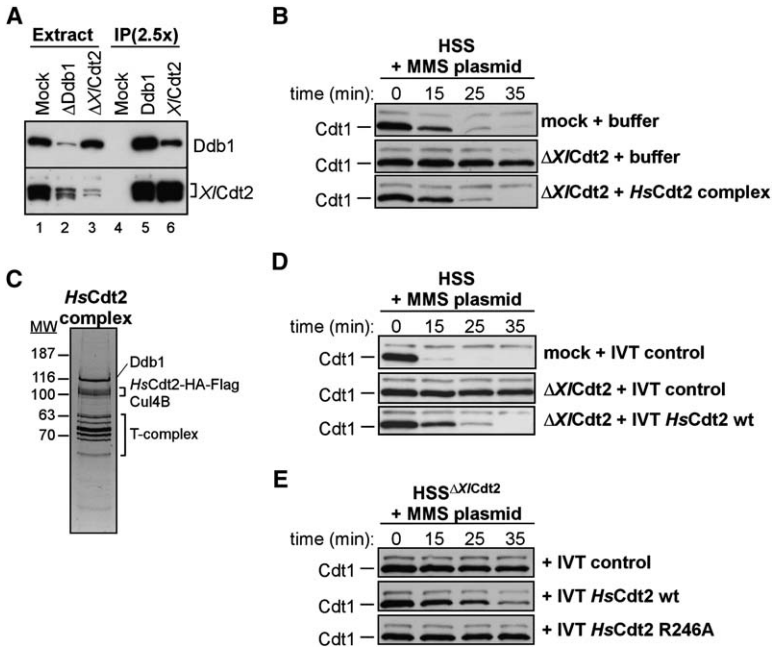

Figure 4. *Xl*Cdt2 Is Required for Damage-Dependent Cdt1 Destruction in *Xenopus* Egg Extracts

(A) Ddb1, *Xl*Cdt2, or preimmune antibodies (mock) were used to immunoprecipitate proteins from egg extract. Supernatant (0.4 μl) (extract) or the immunoprecipitated material from 1.0 μl of extract (IP) was blotted for Ddb1 or *Xl*Cdt2 as indicated.

(B) HSS depleted of *Xl*Cdt2 or mock depleted with preimmune serum was supplemented with 6 ng/μl MMS-treated plasmid and either *Hs*Cdt2-HA-FLAG complex or control buffer. At different times, total Cdt1 levels were examined by Western blotting.

(C) Purified *Hs*Cdt2-HA-FLAG complex was silver stained. The identity of subunits was established by mass spectrometry.

(D) HSS was depleted as in (B) and supplemented with IVT reaction programmed with *Hs*Cdt2 wt expression vector ("IVT *Hs*Cdt2 wt") or unprogrammed IVT reaction ("IVT control") prior to addition of MMS-treated plasmid, and analyzed as in (B).

(E) HSS depleted of *Xl*Cdt2 was supplemented with IVT reaction programmed with *Hs*Cdt2 wt or R246A mutant expression plasmid, or with unprogrammed IVT reaction (IVT control), and processed as in (D). A representative result of three independent experiments is shown.

remained stable after UV treatment, even after 30 min (Figure 3C). We conclude that *Hs*Cdt2 is required for Cdt1 destruction after DNA damage and likely during an unperturbed S phase (see also below).

A Putative *Xenopus* Cdt2 Ortholog Is Required for DNA-Damage-Induced Cdt1 Destruction

Xenopus egg extracts have been used to elucidate the regulation of Cdt1, including the replication dependence and PCNA dependence of its destruction (Arias and Walter, 2005, 2006). Concurrent with the analysis of human DCAFs, we independently identified a requirement for Cdt2 in Cdt1 proteolysis using *Xenopus* egg extracts. Inspired by the role of *Sp*Cdt2 in S phase-dependent and DNA-damage-dependent proteolysis of Spd1, we cloned a putative *Xl*Cdt2 ortholog, which is 44% and 65% similar to *Sp*Cdt2 and *Hs*Cdt2, respectively (data not shown), and it appears to be nuclear (Figure S3). Immunoprecipitation (IP) of Ddb1 from egg extract recovered almost all *Xl*Cdt2 (Figure 4A, lanes 2 and 5), and IP of *Xl*Cdt2 recovered a significant fraction of Ddb1 (Figure 4A, lanes 3 and 6), indicating that all the *Xl*Cdt2 is bound to Ddb1, and that Ddb1 is present in excess.

We first examined the role of *Xl*Cdt2 in DNA-damage-induced destruction of Cdt1. A *h*igh-speed *s*upernatant of *Xenopus* egg cytoplasm (HSS) supports repair synthesis of plasmids damaged with methyl methane sulfonate (MMS; Stokes and Michael, 2003), and, in this setting, proteasome-dependent destruction of Cdt1 is observed (Figure 4B, top panel, and see also Figure S4A). As seen in human cells (Hu and Xiong, 2006; Nishitani et al., 2006; Senga et al., 2006), DNA-damage-induced Cdt1 destruction in HSS is dependent on PCNA and the PIP box motif within Cdt1 (Figures S4B and S4C). To determine whether *Xl*Cdt2 is required for damage-dependent Cdt1 destruction, *Xl*Cdt2 was removed from HSS. Compared to controls, *Xl*Cdt2-depleted extracts were severely compromised for Cdt1 destruction (Figure 4B, compare top and middle panel).

To demonstrate the specificity of *Xl*Cdt2 depletion, it was necessary to rescue the Cdt1 destruction defect with purified Cdt2 protein. We affinity purified *Hs*Cdt2 complexes from human 293T cells (Figure 4C). Mass spectrometry and Western blotting demonstrated the presence of *Hs*Cdt2, Ddb1, and Cul4B (Figure 4C and data not shown). In addition, we found the T complex, a chaperone complex reported to promote assembly of E3s, which also copurifies with *Sp*Cdt2 (Liu et al., 2005). As shown in Figure 4B, bottom panel, the *Hs*Cdt2 complex restored DNA-damage-induced Cdt1 destruction in HSS. To prove that stabilization of Cdt1 in *Xl*Cdt2-depleted extract is solely due to the absence of *Xl*Cdt2, we produced recombinant *Hs*Cdt2 using in vitro translation (IVT). Addition of IVT *Hs*Cdt2, but not control IVT reaction, restored Cdt1 destruction in *Xl*Cdt2-depleted egg extract (Figure 4D). Importantly, mutation of R246 in the WDXR motif in *Hs*Cdt2 rendered *Hs*Cdt2 nonfunctional for Cdt1 degradation (Figure 4E), even though it was produced at levels similar to wild-type *Hs*Cdt2 (data not shown). Together, the experiments in human cells and *Xenopus* egg extracts show that DNA-damage-dependent Cdt1 proteolysis requires the Cul4-Ddb1^{Cdt2} complex.

S Phase Destruction of Cdt1 Requires *Xl*Cdt2

To ask whether *Xl*Cdt2 is required for S phase Cdt1 destruction, we employed a *l*ow speed *s*upernatant of *Xenopus* egg cytoplasm (LSS). LSS assembles sperm chromatin into nuclei that undergo DNA replication and support PCNA-, and Ddb1-dependent Cdt1 destruction (Arias and Walter, 2005, 2006). LSS was depleted with *Xl*Cdt2 antibodies or preimmune serum and

supplemented with sperm chromatin. Cdt1 destruction was impaired in the absence of *Xl*Cdt2 (Figure 5A, third panel), and the defect was reversed by addition of the *Hs*Cdt2 complex (Figure 5A, fourth panel). IVT *Hs*Cdt2 could not be used for rescue because reticulocyte extracts caused nonspecific inhibition of Cdt1 destruction in LSS (data not shown). Depletion of *Xl*Cdt2 had no significant effect on DNA replication, as assessed by loading of the replication initiation factor Cdc45 onto chromatin (Figure 5B) and incorporation of [α-^{32}P]dATP (data not shown).

Replication-dependent ubiquitylation of Cdt1 on chromatin is readily observed in the presence of methylated ubiquitin, a chemically modified form of ubiquitin that is conjugated to target molecules but deficient in polyubiquitin chain formation (Arias and Walter, 2005). Depletion of *Xl*Cdt2 abolished the ubiquitylation of Cdt1 on chromatin, and the effect was partially rescued with the *Hs*Cdt2 complex (Figure 5B). Our data indicate that replication-dependent destruction of Cdt1 in egg extracts requires *Xl*Cdt2.

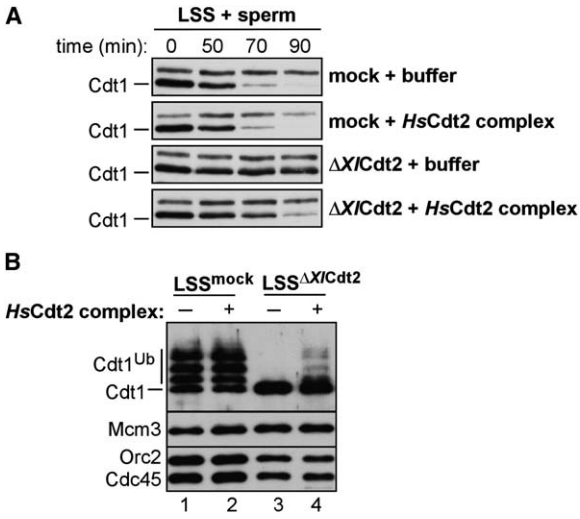

Figure 5. *Xl*Cdt2 Is Required for Replication-Dependent Cdt1 Destruction

Sperm chromatin (10 ng/μL) was added to *Xl*Cdt2- or mock-depleted LSS containing 25 nM rCdt1^{wt}, and *Hs*Cdt2-HA-Flag complex (+*Hs*Cdt2 complex) or control buffer. (A) At the indicated times, 1 μl of extract was blotted for Cdt1. (B) Extracts were also supplemented with 250 μM methylated ubiquitin. Chromatin was isolated after 90 min and blotted with Cdt1, Mcm3, or a mixture of Orc2 and Cdc45 antibodies.

*Xl*Cdt2 Is Recruited to Chromatin via the PIP Box of Cdt1

We showed previously that Ddb1 is recruited to chromatin during replication initiation and postulated that this reflects its involvement in Cdt1 destruction (Arias and Walter, 2006). However, as shown above, Ddb1 interacts with many putative substrate receptors. Therefore, we examined whether recruitment of the Cdt1-specific E3, which contains *Xl*Cdt2, is also replication dependent. As shown in Figure 6A, *Xl*Cdt2 bound to chromatin with similar kinetics as PCNA and the appearance of ubiquitylated Cdt1. Moreover, inhibition of DNA replication by the Cdt1 inhibitor Geminin, the Cdk2 inhibitor p27^{Kip}, or the DNA polymerase α inhibitor aphidicolin blocked *Xl*Cdt2 recruitment to chromatin, as well as Cdt1 ubiquitylation (Figure 6B). Thus, like Ddb1 (Arias and Walter, 2006), *Xl*Cdt2 chromatin binding requires the initiation of DNA replication.

We envisioned two models to explain replication-dependent *Xl*Cdt2 recruitment to chromatin. In one, *Xl*Cdt2 is recruited via Cdt1, which is thought to use its PIP box to bind PCNA at the replication fork (Arias and Walter, 2006). Alternatively, *Xl*Cdt2 may be targeted to chromatin independently of Cdt1. To distinguish between these mechanisms, endogenous Cdt1 was depleted from LSS and replaced with wild-type recombinant Cdt1 (rCdt1^{wt}) or Cdt1 containing a defective PIP box (rCdt1$^{\Delta PIP}$). We have shown previously that rCdt1$^{\Delta PIP}$, while active for DNA replication, fails to get ubiquitylated on chromatin (Arias and Walter, 2006 and Figure 6C, lane 1). DNA synthesis was restored to equal levels by rCdt1^{wt} and rCdt1$^{\Delta PIP}$ (data not shown). Importantly, *Xl*Cdt2 chromatin loading was severely reduced in the presence of rCdt1$^{\Delta PIP}$ compared to rCdt1^{wt}, indicating that association of Cdt1 with PCNA is essential for *Xl*Cdt2 recruitment to chromatin (Figure 6C, compare lanes 1 and 2). In several experiments, we observed similar results for Ddb1 (data not shown), suggesting that recruitment of the entire Cul4-Ddb1^{Cdt2} ligase to chromatin depends on Cdt1. In support of this model, depletion of *Xl*Cdt2 reduced the loading of Ddb1 onto chromatin to the same low level seen when DNA replication was inhibited (Figure 6D). These data are consistent with the idea that docking of Cdt1 onto chromatin bound PCNA creates a signal to recruit Cul4-Ddb1^{Cdt2}.

Depletion of *Hs*Cdt2 from HeLa Cells Leads to G2 Arrest and Rereplication

Overexpression of Cdt1 or depletion of the Cdt1 inhibitor Geminin causes a G2 arrest with rereplication in human cells (Melixetian et al., 2004; Takeda et al., 2005; Zhu et al., 2004). Consistent with these findings, we found that depletion of *Hs*Cdt2 with two independent siRNAs resulted in a dramatic accumulation of cells in the G2/M phase of the cell cycle, as determined by flow cytometry 72 hr after initiation of RNAi (Figure 7A). Interestingly, cells with >4 N DNA content were observed, indicative of rereplication. At this time point, Cdt1 levels were elevated compared to control siRNA-treated cells (Figure 3C, lanes 1, 4, and 7). To more precisely identify the arrest point, we examined the status of histone H3 Ser10 phosphorylation using a phospho-specific antibody (α-pH3). Ser10 phosphorylation occurs initially in G2 at pericentromeric heterochromatin as faint foci and spreads throughout chromatin as cells enter mitosis (Hendzel et al., 1997). We found that cells depleted of *Hs*Cdt2 display a dramatic increase in the number of cells with focal α-pH3 staining, from ~5% in control siRNA-treated cells to 40%–53% in cells treated with two independent *Hs*Cdt2 siRNAs (Figures 7B and 7C). In contrast, the number of strongly α-pH3-positive cells was reduced from ~3% to less than 0.5% (Figures 7B and 7C). These data indicate that depletion of *Hs*Cdt2 leads to accumulation of cells in the G2 phase of the cell cycle. During this analysis, we also noticed that nuclei in *Hs*Cdt2-depleted cells are significantly larger than nuclei from control siRNA-treated

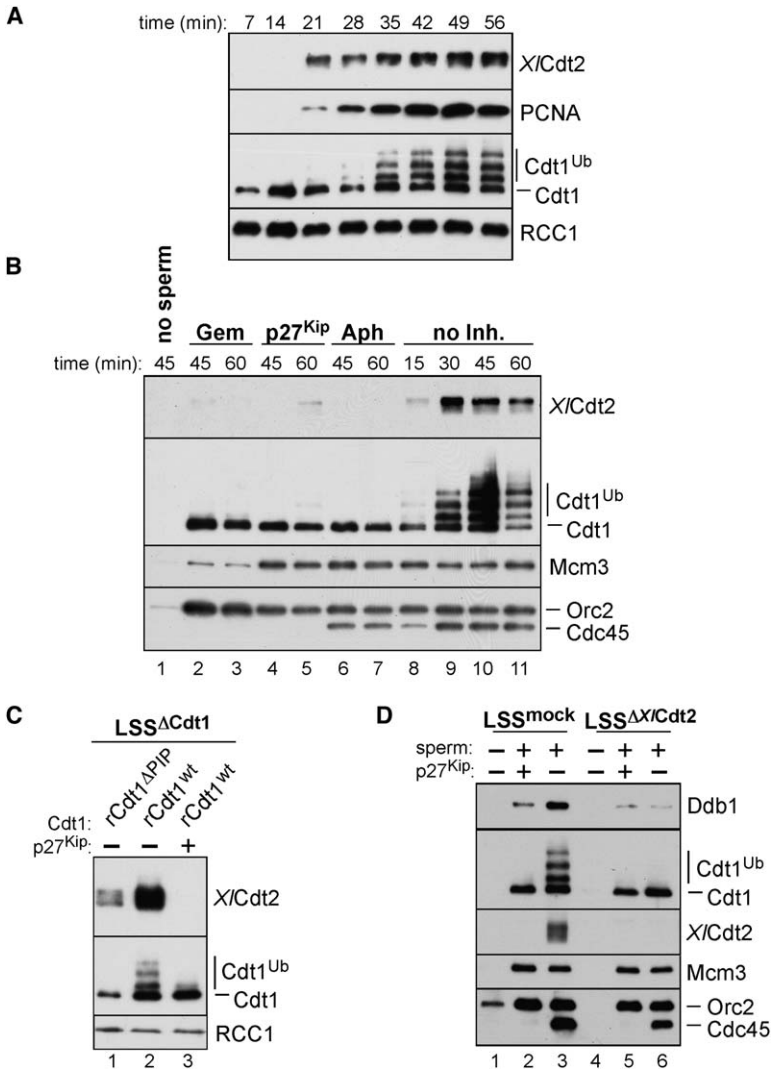

Figure 6. *Xl*Cdt2 Is Recruited to Chromatin During Initiation of Replication and Is Required for Recruitment of Ddb1

(A) Chromatin loading of *Xl*Cdt2. Sperm chromatin (10 ng/μL) was incubated in LSS containing 250 μM methylated ubiquitin. At the indicated times, chromatin was isolated and blotted for *Xl*Cdt2, PCNA, Cdt1, or RCC1 (loading control).

(B) Replication dependence of *Xl*Cdt2 loading. As in (A), except that extract was optionally supplemented with 0.2 μM Geminin, 1 μM $p27^{Kip}$, or 300 μM aphidicolin. Lane 1, no sperm control.

(C) Cdt1 PIP box dependence of *Xl*Cdt2 chromatin loading. Sperm chromatin (10 ng/μl) was added to Cdt1-depleted LSS containing 50 nM $rCdt1^{wt}$ (lanes 2 and 3) or 50 nM $rCdt1^{\Delta PIP}$ (lane 1). Lane 3 also contained 1 μM $p27^{Kip}$. Chromatin was isolated after 60 min and blotted for *Xl*Cdt2, Cdt1, and RCC1 (loading control).

(D) *Xl*Cdt2-dependent chromatin loading of Ddb1. Extract was depleted of *Xl*Cdt2 or mock depleted with the corresponding preimmune serum and optionally supplemented with sperm chromatin (10 ng/μl) and 1 μM $p27^{Kip}$, as indicated. Chromatin was recovered after 70 min and blotted with Ddb1, Cdt1, *Xl*Cdt2, Mcm3, or a mixture of Orc2 and Cdc45 antibodies.

cells (Figures 7B and 7E), consistent with rereplication (Zhu et al., 2004).

Inappropriate rereplication can induce activation of the G2/M DNA damage checkpoint in human cells (Melixetian et al., 2004; Vaziri et al., 2003; Zhu et al., 2004). We found that depletion of *Hs*Cdt2 leads to a dramatic increase in focal γ-H2AX staining indicating activation of the DNA damage checkpoint, with 60%–80% of cells displaying focal γ-H2AX staining compared to <1% in control cells (Figures 7D and 7E). Initiation of the DNA damage response occurs, in part, through activation of the ATM/ATR protein kinases. We found that addition of caffeine, an inhibitor of ATM/ATR kinases, substantially bypassed G2 checkpoint arrest, with >58% of *Hs*Cdt2-depleted cells entering the mitotic state within 3 hr of caffeine addition (Figures 7F and 7G). We conclude that *Hs*Cdt2 depletion leads to Cdt1 accumulation and rereplication, which in turn promotes activation of the G2/M DNA damage checkpoint.

Discussion

Among CRLs, the Cul4 subfamily is the most poorly understood, as the number of such complexes, and their modes of assembly and regulation, are largely unknown. In this work, we identified a diverse family of DCAFs, 14 of which contain WD40 repeats, suggesting their involvement in substrate recruitment. Consistent with this, we demonstrate that DCAF2/*Hs*Cdt2, the human relative of *S. pombe* Cdt2, is required for degradation of the replication licensing protein Cdt1 in human cells in response to DNA damage. Independently, we identified *Xl*Cdt2 as being essential for Cdt1 destruction during DNA replication and after DNA damage in *Xenopus* egg extracts. Cdt1 and Cdt2 were originally identified in *S. pombe* as two structurally unrelated genes whose transcription requires Cdc10 (*C*dc10-*d*ependent *t*ranscripts) (Hofmann and Beach, 1994), but a regulatory relationship between the two proteins has remained hitherto unknown.

DCAFs and Dda1 Interact with Ddb1 in Diverse Ways

Ddb1, which contains three β propellers, is the most complex adaptor protein linking substrate receptors to cullins (Li et al., 2006). Using mutagenesis of conserved residues in Ddb1, we found that the majority of DCAF proteins rely on residues located on the top face of βPC for interaction, the same site employed by the viral SV5 protein, which binds Ddb1 to promote STAT protein

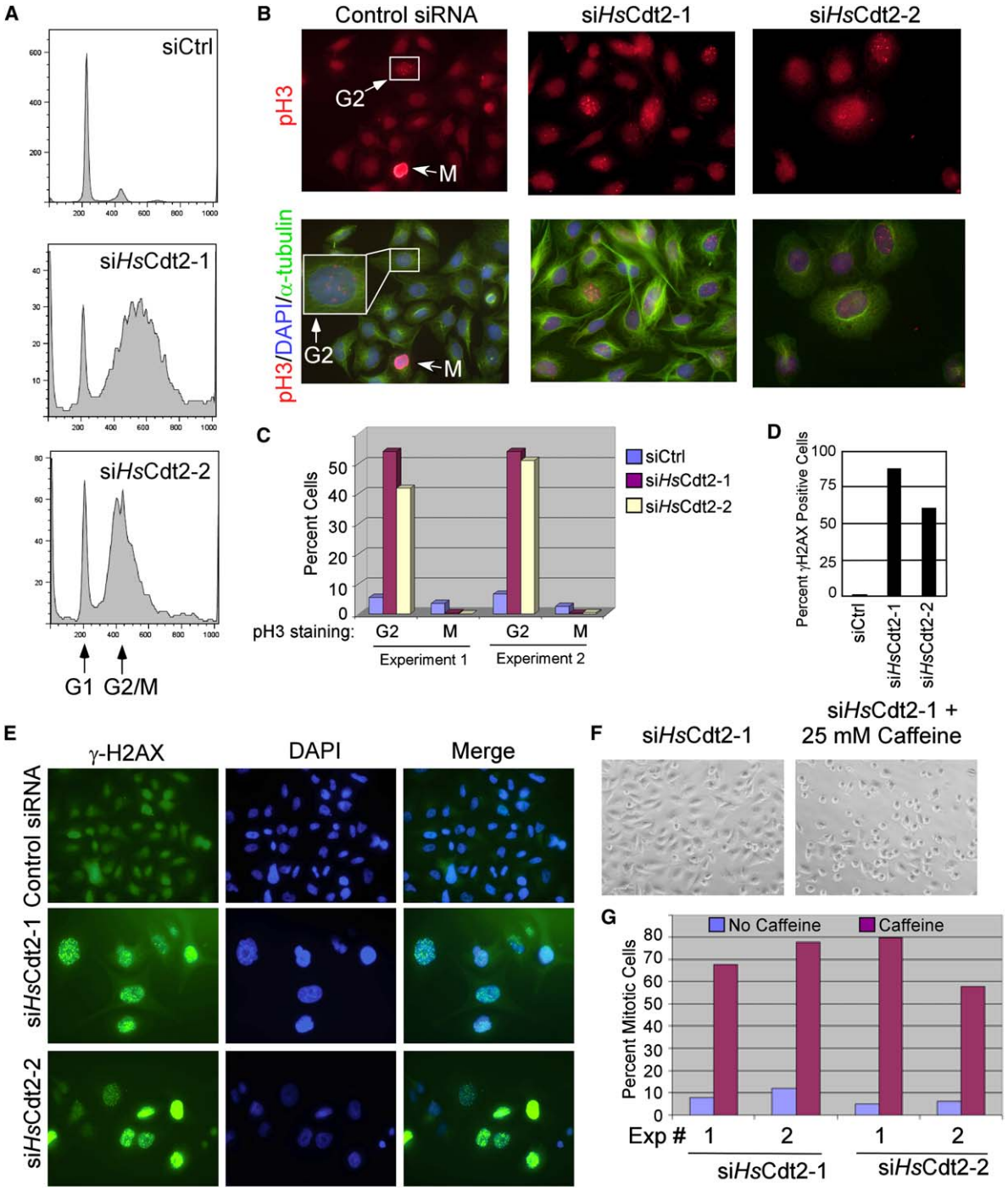

Figure 7. Depletion of *Hs*Cdt2 in HeLa Cells Induces Rereplication, G2 Arrest, and the G2/M DNA Damage Checkpoint

(A) RNAi-treated cells (72 hr) were subjected to flow cytometry.

(B and C) Cells depleted of *Hs*Cdt2 by RNAi transfection arrest in G2. (B) shows representative images of cells stained for phospho-Ser-10 histone H3 (pH3) and α-tubulin, and DAPI to visualize nuclei. In (C), quantification of mitotic pH3 staining is shown for two independent experiments. The number of cells counted ranged from 45 to 693 in 4–15 random fields.

(D and E) Control or si*Hs*Cdt2-transfected cells were subjected to immunofluorescence using γ-H2AX antibodies (green), and cells were counterstained with DAPI to visualize nuclei (E). Quantification of γ-H2AX staining in 90–192 cells in 4–13 random fields is shown (D).

(F and G) *Hs*Cdt2-depleted cells enter mitosis upon addition of caffeine. Cells depleted of *Hs*Cdt2 for 72 hr were incubated with vehicle or 25 mM caffeine for a further 3 hr, and cells were examined using phase contrast microscopy (F). (G) represents the quantification of 105–120 cells in two random fields for the number of cells with mitotic (round) morphology.

ubiquitylation (Li et al., 2006). However, DCAF proteins appear to bind βPC in subtly different ways, as not all DCAFs tested require precisely the same residues in βPC. A subset of Ddb1-associated proteins, including Ddb2, appears not to require residues used by other DCAFs to bind βPC. Nevertheless, it has previously

been demonstrated that Ddb2 competes with SV5 for binding to Ddb1 (Leupin et al., 2003), indicating that they bind similar regions of Ddb1. Thus, it appears that the majority of WD40-containing Ddb1-associated proteins interact with βPC in Ddb1. Interestingly, we found that human Dda1, *D*db1- and *D*et1-*a*ssociated protein-1, required conserved residues in βPA for interaction with Ddb1, suggesting that it plays a role distinct from other DCAF proteins. Together with the finding that Cul4 interacts with βPB (Li et al., 2006) our data suggest that all three β propellers in Ddb1 are used to assemble components of the complex.

The structural basis for Ddb1 binding to diverse WD40-containing proteins is unknown. However, our analysis of DCAFs, Ddb2, and CSA revealed the importance of a WDXR motif. The majority of WD40-containing DCAF proteins contain two WDXR motifs on adjacent internal WD40 repeats. The available data indicate that both tandem WDXR motifs contribute to the interaction with Ddb1. In particular, mutation of the arginine or lysine residues in CSA or DCAF8 in either the first or second motif weakens binding to Ddb1. In addition, mutation of the second WDXR in either *Hs*Cdt2 or DCAF12, or mutation of the single WDXR motif in Ddb2, blocks binding to Ddb1. The fact that these motifs are on the surface of the bottom side of the WD40 propeller leaves the top face available for interaction with substrates, a situation that parallels F-box proteins, which employ the top face of the WD40 propeller to bind substrates (Petroski and Deshaies, 2005). Given that multiple conserved residues in Ddb1 βPC are used in different ways to interact with DCAFs, it seems likely that multiple surfaces in DCAF proteins will likewise be used to interact with Ddb1, probably by employing residues outside of the tandem WDXR motifs.

A survey of human WD40-repeat-containing proteins in GenBank indicates that other members of this protein family not found in our Ddb1 complex by mass spectrometry contain tandem WDXR motifs, raising the possibility that additional DCAF proteins are still to be discovered. Included in this collection are close relatives of several of the genes we identified, including BRWD1 and BRWD3, close relatives of DCAF14; WDR42B, a close relative of DCAF8; and WD40B, a close relative of DCAF12. Further studies are required to determine whether these and other tandem WDXR-containing proteins associate with Ddb1. Such proteins could display tissue-specific expression patterns, or their interaction with Ddb1 could be regulated and therefore not seen in the experiments presented here. It is also possible that additional proteins containing a single identifiable WDXR motif, analogous to Ddb2, might also interact with Ddb1. We speculate that in these cases additional interaction components are used to recognize Ddb1. For example, SV5 employs helical segments near its N terminus to bind Dbd1 (Li et al., 2006). Interestingly, the secondary structure of Ddb2 predicts two α helices located N terminal to its WD40 repeats (Figure S2G, top). We found that deletion of either Helix-1 or Helix-2 largely abolishes interaction between Ddb2 and Ddb1 (Figure S2G). Thus, in the case of Ddb2, sequences outside the WD40 repeats may also contribute to the interaction with Ddb1. In summary, our data indicate that multiple contact points are used both on Ddb1 and on DCAF proteins.

A Universal Mechanism for Cdt1 Destruction

Previous reports suggested that the S phase and DNA damage Cdt1 destruction mechanisms are similar because both require Cul4, Ddb1, PCNA, and the N-terminal PCNA-interaction motif (PIP box) of Cdt1 (Arias and Walter, 2006; Higa et al., 2003; Hu et al., 2004; Hu and Xiong, 2006; Nishitani et al., 2006; Senga et al., 2006). We now show that an additional factor, Cdt2, is required for both pathways. Depletion of *Xl*Cdt2 from egg extracts inhibited Cdt1 destruction during chromosomal DNA replication and in response to DNA damage. In human cells, siRNA knockdown of *Hs*Cdt2 abolished the DNA-damage-induced destruction of Cdt1. While this work was under review, a similar requirement for *Hs*Cdt2 in DNA-damage-induced Cdt1 destruction was proposed (Higa et al., 2006). Furthermore, we found that *Hs*Cdt2 siRNA treatment caused modest Cdt1 accumulation in the absence of external DNA damage, suggesting its destruction during S phase was defective. Together with previous results, our findings suggest that the S phase and DNA damage Cdt1 destruction pathways are identical, involving a common ubiquitin ligase (Cul4-Ddb1^{Cdt2}) and trigger (chromatin bound PCNA).

Based on our previous experiments, including coimmunoprecipitation (CoIP) of Cdt1 with Ddb1 in the absence of chromatin, we proposed that an E3 ligase containing Cul4 and Ddb1 binds to Cdt1 in the nucleoplasm, forming a latent complex that is incompetent for ubiquitin transfer until it docks onto chromatin bound PCNA (Arias and Walter, 2006). The discovery that *Xl*Cdt2 is also involved has led to new insights. Surprisingly, we detected no interaction between Cdt2 and Cdt1 in the absence of chromatin in *Xenopus* egg extracts or human cells (data not shown), and recent experiments indicate that the interaction between Ddb1 and Cdt1, while reproducible, is dependent on the amount of antibody in the IP (data not shown). Therefore, current evidence suggests there is no latent Cdt1:Cul4-Ddb1^{Cdt2} complex in the absence of chromatin. Instead, our data suggest that Cdt1 and its E3 ligase interact directly on chromatin. Thus, the recruitment of *Xl*Cdt2 to chromatin in S phase requires replication initiation and the interaction of Cdt1 with PCNA. Furthermore, the chromatin loading of Ddb1 requires *Xl*Cdt2. From these results, we infer that the binding of Cdt1 to PCNA on chromatin generates a signal that recruits the Cul4-Ddb1^{Cdt2} ligase. We speculate that the interaction of Cdt1's PIP box with chromatin bound PCNA creates a surface with high affinity for Cul4-Ddb1^{Cdt2}. Consistent with this model, a short peptide of Cdt1 encompassing the PIP box motif is sufficient to confer PCNA-dependent destruction in human cells (Senga et al., 2006; Nishitani et al., 2006). Thus, Cdt1 ubiquitylation is controlled at the level of binding to its E3 ligase, and this event is temporally regulated due to its dependence on chromatin bound PCNA, an S phase-specific and DNA-damage-specific structure.

An important question addresses whether the Cul4-Ddb1^{Cdt2} ligase binds to Cdt1 via Cdt2. By analogy with the direct binding of *Sp*Cdt2 to its substrate Spd1 (Liu et al., 2005), we expect this to be the case. However, because we believe that the interaction only occurs on chromatin bound PCNA, and because Cdt1 and Cdt2 expressed in bacteria and insect cells are prone to

aggregation, it has been difficult to test directly whether Cdt2 is the substrate receptor for Cdt1.

Effects of *Hs*Cdt2 Depletion on the Cell Cycle

Inhibition of Cdt1 activity during S phase by Geminin and proteolysis is essential to maintain once-per-cell-cycle regulation of DNA replication in metazoans (Blow and Dutta, 2005). In addition to the PCNA-dependent Cdt1 destruction pathway, mammalian cells also employ SCF^{Skp2}-mediated Cdt1 destruction, which depends on phosphorylation of Cdt1 by Cdk2 (Li et al., 2003; Nishitani et al., 2006; Senga et al., 2006). Deregulation of Cdt1 in mammalian cells via Cdt1 overexpression or knockdown of Geminin is sufficient to cause rereplication in S phase, which in turn causes DNA damage and checkpoint-dependent cell cycle arrest in G2 (Melixetian et al., 2004; Zhu et al., 2004).

We found that *Hs*Cdt2 depletion produces a remarkably exact phenocopy of Cdt1 overexpression/Geminin depletion, in that cells arrest in G2 phase with DNA damage and >4 N DNA content. Although in *Hs*Cdt2-depleted cells Cdt1 is only modestly elevated compared to controls (Figures 3B and 3D), these cells are effectively arrested in G2, when Cdt1 is normally absent (Figure 7A). Therefore, silencing *Hs*Cdt2 causes a dramatic overexpression of Cdt1 in G2 cells. Given the multiple mechanisms that are proposed to inhibit Cdt1 function in human cells, it is not immediately obvious why depletion of *Hs*Cdt2 should, by itself, induce rereplication. However, the rereplication observed in human cells upon *Hs*Cdt2 silencing indicates that the $Cul4\text{-}Ddb1^{Cdt2}$ destruction pathway is essential and implies that SCF^{Skp2} is not sufficient to functionally neutralize Cdt1. This result is in agreement with the previous finding that cosilencing of both Cul4A and Cul4B is sufficient to cause Cdt1 accumulation in a significant number of cells in S/G2 phases (Nishitani et al., 2006). We speculate that, in the absence of *Hs*Cdt2, Cdt1 accumulates during S phase, eventually exceeding the concentration of Geminin, thus triggering rereplication, DNA damage, and checkpoint activation. The checkpoint may, in turn, downregulate Cdk activity, leading to inhibition of the SCF^{Skp2} pathway and to enhanced Cdt1 stabilization.

DCAF Proteins and Cul4-Ddb1 Function

To date, the functions of Cul4-Ddb1 that have been uncovered are closely linked with chromatin biology, including ubiquitylation of histones H3 and H4 and the DNA repair factor XPC by $Cul4\text{-}Ddb1^{Ddb2}$, ubiquitylation of the transcription-coupled repair factor CSB by $Cul4\text{-}Ddb1^{CSA}$ (Groisman et al., 2006; Sugasawa et al., 2005; Wang et al., 2006), and, now, PCNA-dependent destruction of Cdt1 by $Cul4\text{-}Ddb1^{Cdt2}$. We speculate that additional links to chromatin function and control of DNA damage will emerge from the analysis of further DCAFs.

Experimental Procedures

Plasmids

Open reading frames were obtained using available EST clones or by RT-PCR from mRNA isolated from 293T cells, and occasionally from the Human Orfeome Collection (provided by Marc Vidal, Dana-Farber Cancer Institute). For PCR primers, see Table S1. Cloned PCR products in pENTR/D-TOPO (Invitrogen) were sequenced prior to recombination into the indicated epitope tag expression vector. Mutations were generated using PCR-based mutagenesis.

Proteomic Analysis of the Ddb1 Complex

MSCV-Flag-HA-Ddb1 ($puro^R$) was packaged and used to transduce 293T cells using puromycin (1 μg/ml). Thirty 15 cm dishes of control cells or cells expressing Flag-HA-Ddb1 were harvested and lysed in extraction buffer (50 mM Tris-HCl [pH 7.5], 150 mM NaCl, 1% nonidet P40, 10 mM β-glycerol phosphate, 10 mM p-nitrophenyl phosphate, 0.1 μM okadaic acid, and 10 mM NaF), and the lysate was cleared. The extract was incubated with 250 μl of α-Flag resin (3 hr at 4°C), the complex was eluted with Flag peptide (500 μg/ml, 3 × 30 min, 4°C in extraction buffer), and the supernatant was applied to α-HA resin (50 μl, 2 hr, at 4°C). Complexes were eluted with HA peptide (500 μg/ml, 3 × 30 min, 25°C in extraction buffer) and subjected to mass spectrometry after SDS-PAGE.

To examine Ddb1/DCAF interactions, plasmids were cotransfected into 293T cells (maintained in DMEM supplemented with 10% fetal bovine serum with 5% CO_2) in 6-well dishes using Lipofectamine 2000 (Invitrogen). Cells were lysed prior to immunopurification and immunoblotting.

Egg Extracts and Miscellaneous

Chromatin isolations, depletions, and preparation of LSS, HSS, and NPE were performed as described (Arias and Walter, 2005, 2006). MMS-damaged pBluescript was generated as described (Stokes and Michael, 2003).

Protein Expression and Purification

Recombinant Cdt1 was purified as described (Arias and Walter, 2005). Recombinant human PCNA was a gift from John Pascal and Tom Ellenberger (Harvard Medical School). Recombinant *Hs*Cdt2-HA-Flag complexes were affinity purified from 293T cells essentially as described for the Ddb1 complex and subjected to mass spectrometry. In rescue experiments, *Hs*Cdt2 complex was added to a final concentration of ~1 ng/μL. TNT T7-coupled in vitro-translated *Hs*Cdt2 (wt and R246A) (Promega) was added to HSS at a 1:10 dilution (Figure 4D) or 1:6 dilution (Figure 4E). The IVT mix was incubated in HSS for 10 min at 22°C, followed by 20 min on ice prior to addition of MMS plasmid and 25 nM $rCdt1^{wt}$. For experiments comparing wt versus R246A *Hs*Cdt2, proteins were labeled with ^{35}S-methionine and quantified by phosphoimager analysis after SDS-PAGE.

Immunological Methods

A C-terminal fragment of *Xl*Cdt2 (amino acids 321–711) or a fragment of *Xl*DCAF1 (amino acids 1296–1507) was cloned into pET-DUET-1 (Novagen/EMD), expressed in *E. coli*, purified from inclusion bodies, and injected into rabbits. Immunoprecipitations were as described (Arias and Walter, 2006), except that starting extract was 1:1 HSS and NPE diluted with two volumes of ELB salts (50 mM KCl, 2.5 mM $MgCl_2$, 10 mM HEPES [pH 7.7]). For detection of *Hs*Cdt2, α-*Xl*Cdt2 antibodies were affinity purified using immobilized *Hs*Cdt2. For Figure 1D, α-*Xl*DCAF1 antibodies were used. All other *Xenopus* antibodies have been described (Arias and Walter, 2006). α-*Hs*Cdt1 was provided by Xiaohua Wu (UCSD). Other antibodies are commercial: α-Ddb1 (Zymed); α-Cul4 (Rockland); α-Flag (Sigma) and α-HA (Santa Cruz Biotechnology); and α-γ-H2AX and α-phospho-S10-histone H3 (Cell Signaling Technologies). For immunofluorescence, cells were fixed with paraformaldehyde (4%) for 10 min at room temperature, permeabilized with 0.5% Triton X-100, and subjected to indirect immunofluorescence. Nuclei were stained with DAPI. Imaging was with an Axiovert 200 microscope and a Hammumatsu camera.

RNAi

siRNAs (240 pmol) (Table S1) from either Invitrogen or Dharmacon were transfected into HeLa cells (in 6-well dishes) using oligofectamine. After 48–72 hr, cells were left untreated or were UV irradiated (20 J/m^2) prior to lysis in SDS lysis buffer. Extracts were subjected to SDS-PAGE and immunoblotting. RNAi-treated cells were fixed for flow cytometry using propidium iodide to label DNA or were subjected to immunofluorescence.

Supplemental Data

Supplemental Data include four figures and one table and can be found with this article online at http://www.molecule.org/cgi/content/full/23/5/709/DC1/.

Acknowledgments

We thank Xiaohua Wu (UCSD) for α-Cdt1, Marc Vidal (Dana-Farber Cancer Institute) for the Human Orfeome Collection, and Matt Michael (Harvard University) for communicating to us the in vitro Cdt1 destruction assay. We thank Steve Gygi and Judit Villen (Harvard Medical School) for mass spectrometry analysis of *Hs*Cdt2 complexes and John Asara (Beth Israel Deaconess Medical Center/Harvard Medical School Department of Pathology Mass Proteomics Facility) for analysis of Ddb1 complexes. We thank Ning Zheng (University of Washington) for communicating results prior to publication. E.E.A. is a Howard Hughes Medical Institute predoctoral fellow. J.C.W. was supported by an American Cancer Society grant (106201), and J.W.H by National Institutes of Health grants AG11085 and GM54137, and by a gift from Merck, Inc.

Received: July 14, 2006
Revised: August 15, 2006
Accepted: August 16, 2006
Published: August 31, 2006

References

Arias, E.E., and Walter, J.C. (2005). Replication-dependent destruction of Cdt1 limits DNA replication to a single round per cell cycle in *Xenopus* egg extracts. Genes Dev. *19*, 114–126.

Arias, E.E., and Walter, J.C. (2006). PCNA functions as a molecular platform to trigger Cdt1 destruction and prevent re-replication. Nat. Cell Biol. *8*, 84–90.

Bai, C., Sen, P., Hofmann, K., Ma, L., Goebl, M., Harper, J.W., and Elledge, S.J. (1996). SKP1 connects cell cycle regulators to the ubiquitin proteolysis machinery through a novel motif, the F-box. Cell *86*, 263–274.

Blow, J.J., and Dutta, A. (2005). Preventing re-replication of chromosomal DNA. Nat. Rev. Mol. Cell Biol. *6*, 476–486.

Cao, H., Williams, C., Carter, M., and Hegele, R.A. (2004). CKN1 (MIM 216400): mutations in Cockayne syndrome type A and a new common polymorphism. J. Hum. Genet. *49*, 61–63.

Chen, X., Zhang, Y., Douglas, L., and Zhou, P. (2001). UV-damaged DNA-binding proteins are targets of CUL-4A-mediated ubiquitination and degradation. J. Biol. Chem. *276*, 48175–48182.

Groisman, R., Kuraoka, I., Chevallier, O., Gaye, N., Magnaldo, T., Tanaka, K., Kisselev, A.F., Harel-Bellan, A., and Nakatani, Y. (2006). CSA-dependent degradation of CSB by the ubiquitin-proteasome pathway establishes a link between complementation factors of the Cockayne syndrome. Genes Dev. *20*, 1429–1434.

Hendzel, M.J., Wei, Y., Mancini, M.A., Van Hooser, A., Ranalli, T., Brinkley, B.R., Bazett-Jones, D.P., and Allis, C.D. (1997). Mitosis-specific phosphorylation of histone H3 initiates primarily within pericentromeric heterochromatin during G2 and spreads in an ordered fashion coincident with mitotic chromosome condensation. Chromosoma *106*, 348–360.

Higa, L.A., Mihaylov, I.S., Banks, D.P., Zheng, J., and Zhang, H. (2003). Radiation-mediated proteolysis of CDT1 by CUL4-ROC1 and CSN complexes constitutes a new checkpoint. Nat. Cell Biol. *5*, 1008–1015.

Higa, L.A., Banks, D., Wu, M., Kobayashi, R., Sun, H., and Zhang, H. (2006). L2DTL/CDT2 interacts with the CUL4/DDB1 complex and PCNA and regulates CDT1 proteolysis in response to DNA damage. Cell Cycle *5*, 1675–1680.

Hofmann, J.F., and Beach, D. (1994). cdt1 is an essential target of the Cdc10/Sct1 transcription factor: requirement for DNA replication and inhibition of mitosis. EMBO J. *13*, 425–434.

Hu, J., and Xiong, Y. (2006). An evolutionarily conserved function of proliferating cell nuclear antigen for cdt1 degradation by the cul4-ddb1 ubiquitin ligase in response to DNA damage. J. Biol. Chem. *281*, 3753–3756.

Hu, J., McCall, C.M., Ohta, T., and Xiong, Y. (2004). Targeted ubiquitination of CDT1 by the DDB1–CUL4A-ROC1 ligase in response to DNA damage. Nat. Cell Biol. *6*, 1003–1009.

Kapetanaki, M.G., Guerrero-Santoro, J., Bisi, D.C., Hsieh, C.L., Rapic-Otrin, V., and Levine, A.S. (2006). The DDB1-CUL4ADDB2 ubiquitin ligase is deficient in xeroderma pigmentosum group E and targets histone H2A at UV-damaged DNA sites. Proc. Natl. Acad. Sci. USA *103*, 2588–2593.

Leupin, O., Bontron, S., and Strubin, M. (2003). Hepatitis B virus X protein and simian virus 5 V protein exhibit similar UV-DDB1 binding properties to mediate distinct activities. J. Virol. *77*, 6274–6283.

Li, X., Zhao, Q., Liao, R., Sun, P., and Wu, X. (2003). The SCF(Skp2) ubiquitin ligase complex interacts with the human replication licensing factor Cdt1 and regulates Cdt1 degradation. J. Biol. Chem. *278*, 30854–30858.

Li, T., Chen, X., Garbutt, K.C., Zhou, P., and Zheng, N. (2006). Structure of DDB1 in complex with a paramyxovirus V protein: viral hijack of a propeller cluster in ubiquitin ligase. Cell *124*, 105–117.

Liu, C., Poitelea, M., Watson, A., Yoshida, S.H., Shimoda, C., Holmberg, C., Nielsen, O., and Carr, A.M. (2005). Transactivation of Schizosaccharomyces pombe cdt2+ stimulates a Pcu4-Ddb1-CSN ubiquitin ligase. EMBO J. *24*, 3940–3951.

Melixetian, M., Ballabeni, A., Masiero, L., Gasparini, P., Zamponi, R., Bartek, J., Lukas, J., and Helin, K. (2004). Loss of Geminin induces rereplication in the presence of functional p53. J. Cell Biol. *165*, 473–482.

Nishitani, H., Taraviras, S., Lygerou, Z., and Nishimoto, T. (2001). The human licensing factor for DNA replication Cdt1 accumulates in G1 and is destabilized after initiation of S-phase. J. Biol. Chem. *276*, 44905–44911.

Nishitani, H., Sugimoto, N., Roukos, V., Nakanishi, Y., Saijo, M., Obuse, C., Tsurimoto, T., Nakayama, K.I., Nakayama, K., Fujita, M., et al. (2006). Two E3 ubiquitin ligases, SCF-Skp2 and DDB1-Cul4, target human Cdt1 for proteolysis. EMBO J. *25*, 1126–1136.

Petroski, M.D., and Deshaies, R.J. (2005). Function and regulation of cullin-RING ubiquitin ligases. Nat. Rev. Mol. Cell Biol. *6*, 9–20.

Pickart, C.M. (2004). Back to the future with ubiquitin. Cell *116*, 181–190.

Senga, T., Sivaprasad, U., Zhu, W., Park, J.H., Arias, E.E., Walter, J.C., and Dutta, A. (2006). PCNA is a co-factor for Cdt1 degradation by CUL4/DDB1 mediated N-terminal ubiquitination. J. Biol. Chem. *281*, 6246–6252.

Stokes, M.P., and Michael, W.M. (2003). DNA damage-induced replication arrest in *Xenopus* egg extracts. J. Cell Biol. *163*, 245–255.

Sugasawa, K., Okuda, Y., Saijo, M., Nishi, R., Matsuda, N., Chu, G., Mori, T., Iwai, S., Tanaka, K., Tanaka, K., and Hanaoka, F. (2005). UV-induced ubiquitylation of XPC protein mediated by UV-DDB-ubiquitin ligase complex. Cell *121*, 387–400.

Takeda, D.Y., Parvin, J.D., and Dutta, A. (2005). Degradation of Cdt1 during S phase is Skp2-independent and is required for efficient progression of mammalian cells through S phase. J. Biol. Chem. *280*, 23416–23423.

Vaziri, C., Saxena, S., Jeon, Y., Lee, C., Murata, K., Machida, Y., Wagle, N., Hwang, D.S., and Dutta, A. (2003). A p53-dependent checkpoint pathway prevents rereplication. Mol. Cell *11*, 997–1008.

Wang, H., Zhai, L., Xu, J., Joo, H.Y., Jackson, S., Erdjument-Bromage, H., Tempst, P., Xiong, Y., and Zhang, Y. (2006). Histone H3 and H4 ubiquitylation by the CUL4-DDB-ROC1 ubiquitin ligase facilitates cellular response to DNA damage. Mol. Cell *22*, 383–394.

Wertz, I.E., O'Rourke, K.M., Zhang, Z., Dornan, D., Arnott, D., Deshaies, R.J., and Dixit, V.M. (2004). Human De-etiolated-1 regulates c-Jun by assembling a CUL4A ubiquitin ligase. Science *303*, 1371–1374.

Zhang, S., Feng, Y., Narayan, O., and Zhao, L.J. (2001). Cytoplasmic retention of HIV-1 regulatory protein Vpr by protein-protein interaction with a novel human cytoplasmic protein VprBP. Gene *263*, 131–140.

Zheng, N., Schulman, B.A., Song, L., Miller, J.J., Jeffrey, P.D., Wang, P., Chu, C., Koepp, D.M., Elledge, S.J., Pagano, M., et al. (2002). Structure of the Cul1-Rbx1-Skp1-F boxSkp2 SCF ubiquitin ligase complex. Nature *416*, 703–709.

Zhong, W., Feng, H., Santiago, F.E., and Kipreos, E.T. (2003). CUL-4 ubiquitin ligase maintains genome stability by restraining DNA-replication licensing. Nature *423*, 885–889.

Zhu, W., Chen, Y., and Dutta, A. (2004). Rereplication by depletion of geminin is seen regardless of p53 status and activates a G2/M checkpoint. Mol. Cell. Biol. *24*, 7140–7150.